*Geomagnetism and Aeronomy, Vol. 37, No. 4, 1997, pp. 456–462. Translated from Geomagnetizm i Aeronomiya, Vol. 37, No. 4, 1997, pp. 86–94.*


# Dynamics of Medium-Scale Traveling Ionospheric Disturbances Based on the Data of Transionospheric Sounding

**E. L. Afraimovich, O. N. Boitman, E. I. Zhovty, A. D. Kalikhman, and T. G. Pirog**
*Institute of Solar–Terrestrial Physics, Siberian Division, Russian Academy of Sciences, P.O. Box 4026, Irkutsk, 664033 Russia*
Received May 6, 1996; in final form, November 11, 1996

**Abstract**—The dynamics of medium-scale traveling ionospheric disturbances is compared to small-scale annual variations in polarization, arrival angles, and scintillation of the 136-MHz radio signal from the geostationary satellite *ETS 2* measured in Irkutsk. The diurnal observations agree with the model of the filtering of atmospheric gravity waves by the neutral wind. Two groups of disturbances with opposite directions of phase velocities, close to the direction of small-scale traveling ionospheric disturbances and the normal to the magnetic vector shadow in the antenna array plane, are observed at night. The results obtained allow us to suppose that night-time medium-scale irregularities are frozen in the magnetic field as small-scale ones.

## INTRODUCTION

The study of ionospheric processes, associated with the propagation of atmospheric gravity waves (AGV) and recorded as medium-scale traveling ionospheric disturbances (TID) with typical dimensions of about 100 km, is of great interest to the physics of the ionosphere and radiowave propagation in the ionosphere. One of the interesting AGV manifestations at ionospheric altitudes, which is related to TID filtering by the neutral wind, has been studied for the last two decades [1–10].

The geomagnetic field is another important factor, responsible for the structure and dynamics of ionospheric irregularities. The magnetic field most perceptibly affects the structure and dynamics of small-scale irregularities with characteristic dimensions of 0.1 to 1.0 km. The measurements of the velocity and anisotropy of these irregularities during transionospheric radio sounding at midlatitudes indicated that the irregularities are extended along the geomagnetic field lines and travel perpendicular to this direction [11–13].

However, the data of the observations of not only small-scale but also medium-scale (10–100 km) field-aligned irregularities appeared recently [14]. The relationship between medium-scale TID and small-scale irregularities was found during the study of *F*-scattering in the ionosphere, resulting in a separation of traces in ionograms [15].

This work is aimed at studying the dynamics of medium-scale TID, as compared to that of small-scale irregularities, on the basis of the data of continuous round-the-clock measurements of polarization, arrival angles, and scintillation of the 136-MHz radio signal from the geostationary satellite *ETS 2*, collected by us in Irkutsk (52.5° N, 102.5° E) from December 1989 to December 1990 [16].

## DYNAMIC CHARACTERISTICS OF MEDIUM- AND SMALL-SCALE IRREGULARITIES

The dynamic characteristics of medium-scale TID were analyzed on the basis of statistics of daily and seasonal variations in the following characteristics of the transionospheric radio signal, obtained at a time interval of 30 s with the help of algorithms described earlier [16–18].

(1) Total electron content (TEC) in a vertical column $I(t)$, obtained on the basis of polarization plane rotation measured to an accuracy of an unknown constant component related to night ionization.

(2) Variations in the phase time derivative $\phi'_t(t)$ determined during the measurements of the Doppler shift of frequency.

(3) Variations in the phase spatial derivatives $\phi'_x(t)$ and $\phi'_y(t)$ proportional to changes in the directrix of arrival angles and calculated during measurements of phase differences between signals at spaced antennas.

(4) Variations in velocity $v$ and direction $\psi$ of phase front travel.

Continuous sets of the above parameters were filtered in the range of periods 30–60 min most typical of medium-scale TID.

The data on TID dynamics are obtained using the statistical method for determining a velocity $v$ and direction $\psi$ of radio signal phase-front travel in the antenna array plane [17, 18], which was developed by us and generalized the method proposed in [7].

At each specific instant $t$, the simplest space–time phase variations $\phi(x, y, t)$ of a transionospheric radio signal, proportional to TEC variations $\Delta I(x, y, t)$ in the ionosphere, can be represented as a phase front moving relative to a planar ground

$$\begin{aligned}\phi(x, y, t) &= k\Delta I(x, y, t) \\ &= \phi_t'(t)\Delta t + \phi_x'(t)\Delta x + \phi_y'(t)\Delta y,\end{aligned} \quad (1)$$

where $k$ is a proportionality factor. We assume that distances $\Delta x$, $\Delta y$ between receiving antennas are considerably shorter than the characteristic spatial scale of a disturbance, and that the time interval $\Delta t$ between readings is much less than the temporal scale of the disturbance, so that the effect of second derivatives can be ignored.

Then, at each specific instant, phase front velocity $V(t)$ and direction $\psi(t)$ can be determined as

$$\begin{aligned}W_y(t) &= \phi_y'(t)/\phi_t'(t); \quad W_x(t) = \phi_x'(t)/\phi_t'(t); \\ V(t) &= 1/\sqrt{W_x^2(t) + W_y^2(t)}; \\ \psi(t) &= \arctan[W_x(t)/W_y(t)].\end{aligned} \quad (2)$$

The simplest model of a solitary planar traveling wave of a TEC disturbance is a particular case of (1)

$$\Delta I = \delta I_0 \sin\varphi(t) = \delta I_0 \sin(k_x x + k_y y - \Omega t + \varphi_0), \quad (3)$$

where $I_0$ is an undisturbed TEC value; $\delta$, $k_x$, $k_y$, and $\Omega$ are amplitude, $x$ and $y$ projections of the wave vector, and angular frequency of disturbance; $T = 2\pi/Q$ and $\Lambda = 2\pi/|k|$ are time interval and wavelength; and $\varphi_0$ is the initial phase of the disturbance.

In is shown [7] that, during transionospheric sounding, TEC disturbances $\delta I(x, y, t)$ duplicate the horizontal component of the corresponding disturbance of electron density $\delta N(x, y, z, t)$ and can be used in TID azimuth ($\psi$) measurements (to an accuracy of 180°). Our method makes it possible not only to eliminate azimuth $\psi$ indefiniteness but also to determine travel speed $V$.

In this work, the instantaneous values of $V$ and $\psi$, determined at a time interval of 30 s, are used to form the azimuth $P(\psi)$ and velocity $P(V)$ distributions over a time interval of about 2 h. In an ideal case of solitary planar traveling wave (3), transformations (2) give time-constant values of azimuth and velocity, and the distribution functions have a clearly defined maximum. More complex distribution functions are also possible in the experiment.

Certain data of the continuous annual cycle of observations were eliminated from the subsequent analysis mainly because of interruptions in satellite transmitter operation. The results of statistical data manipulation below, correspond to the winter, spring, summer, and autumn 1989–1990 (17, 35, 20, and 43 days, respectively). In the period of observations considered, the geomagnetic conditions were characterized by medium values of $K_p$ index with the average value of about 2.36. In individual days, specifically, during the strong magnetic storm on April 10 1990, the geomagnetic activity index exceeded 6.0.

To compare the dynamics of medium-scale TID and small-scale irregularities by means of classical correlation analysis, we treated the records of amplitude scintillations at spaced receivers for identical time intervals [16].

The daily variations in space–time phase characteristics of the radio signal from *ETS 2* in the range of periods 30–60 min on November 15 1990 are plotted in Fig. 1 ($K_p$ = 0.76). The daily variations of TEC in a vertical column (Fig. 1a) are typical of a winter day with quiet magnetic conditions: the amplitude is up to 35 × $10^{16}$ electron/m$^2$, and the zero value corresponds to a minimum TEC value at night.

The variations in TEC a day after the strong magnetic disturbance on April 11 1990 ($K_p$ = 5.3) are substantially different (Fig. 1d). On that day, maximum TEC value in daytime was not higher than 15 × $10^{16}$ electron/m$^2$, though it was about 30 × $10^{16}$ electron/m$^2$ two days before. The TEC variations are similar even in summer days with quiet magnetic conditions, which agrees with the data of other researchers.

Figure 1 shows the daily variations in the instantaneous values of $\psi(t)$ and $V(t)$ for series $\phi_t'(t)$, $\phi_x'(t)$, and $\phi_y'(t)$ on (b, c) November 15, 1990 and (e, f) April 11, 1990. It is seen that the magnetically quiet day is characterized by a regular clockwise rotation of direction $\psi$ in the azimuth interval 130°–220°. In the magnetically active day, we can hardly distinguish any regularity in direction $\psi$ variations.

## TID DYNAMICS

Figure 2 displays total azimuth $P(\psi)$ and velocity $P(V)$ distributions of medium-scale TID and small-scale irregularities, plotted on the basis of phase characteristics and amplitude scintillations of the *ETS 2* signal measured during 115 days of 1989–1990: (a) in the daytime with the use of 138 995 thirty-second intervals, (b) at night with the use of 149 842 time intervals, and (c) at night on 922 six-minute intervals.

The daily $P(\psi)$ distribution (Fig. 2a, left plate) has a symmetric form and an average value of 160°. We should note that a majority of $\psi$ values range between 90° and 230°. The velocities $P(V)$ are also symmetrically distributed with the mean value of 133 m/s (Fig. 2a, right panel).

The data of night-time measurements are substantially different. The $P(\psi)$ distribution of medium-scale TID (Fig. 2b, left panel) has two clearly defined, symmetric, principal maxima with most probable values of about 35° and 215° and an insignificant spread in values (within ±10°). The distribution of directions of small-scale irregularities has a similar form (Fig. 2c, left plate). The only difference is that this plot is asymmetric with a more pronounced southwestward direction ($\psi$ = 240°), exceeding the corresponding value for TID by 15° on average. It is also interesting that the

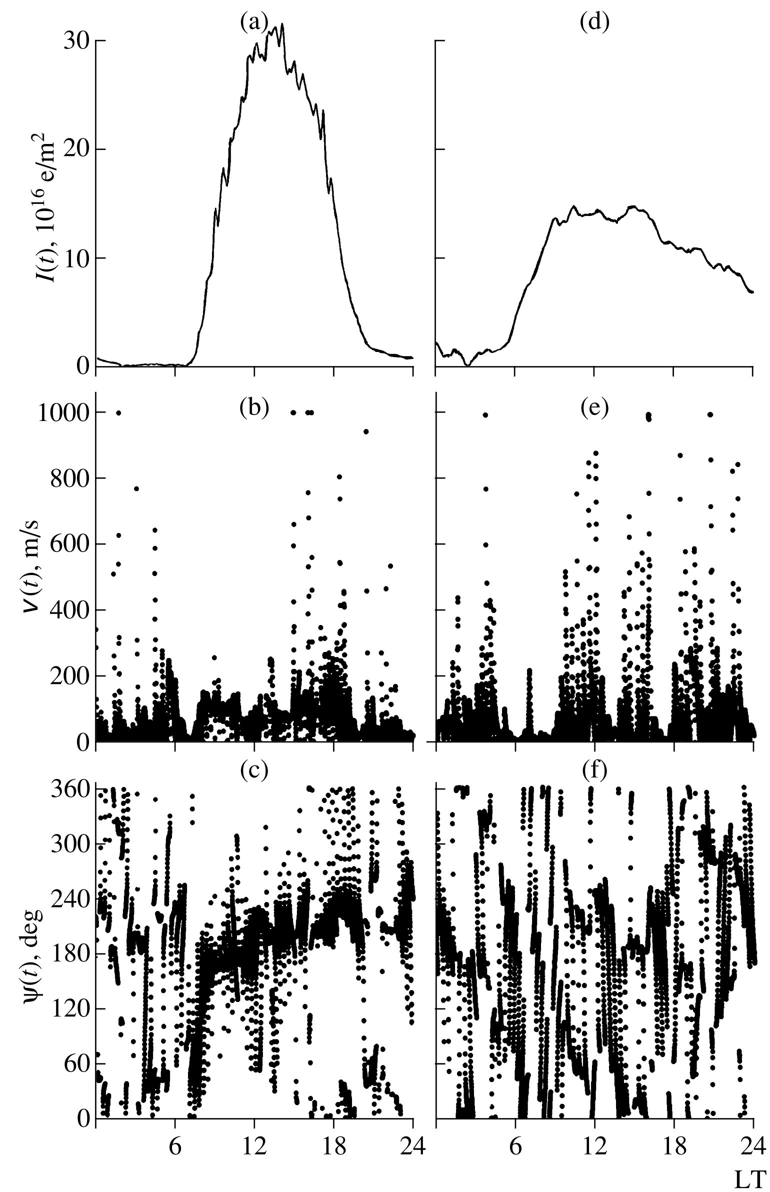


**Fig. 1.** Daily variations in space-time phase characteristics of the radio signal from *ETS 2* for magnetically quiet conditions on November 15 (left image) and during the strong magnetic disturbance on April 11 1990 (right image): (a) and (d) total electron content; (b) and (e) velocity of the phase front travel; and (c) and (f) travel azimuth counted clockwise from a northern direction.

$P(V)$ distributions of medium- and small-scale irregularities show close average values (61 and 46 m/s, respectively) and forms.

For qualitative analysis of TID hourly dynamics, the $V$ and $\psi$ values, determined at a thirty-second interval, were averaged on a current two-hour interval (240 readings), and an average value was assigned to a specific daytime. While considering seasonal variations in TID, we averaged hourly average values for all days in a corresponding season. Figure 3 represents the hourly values of azimuth $\psi(t)$ and velocity $V(t)$ plotted as vectors in polar coordinates on the sweeps for the local time of the day during (a) winter, (b) autumn, (c) spring, and (d) summer. An arrow length corresponds to an absolute value of velocity.

The analysis of the autumn and winter vector diagrams indicates that, at night, the number of oppositely directed displacements with most probable azimuths about 35° and 215° is equal. In the morning and daytime hours, the TIDs rapidly change their eastward direction to a southeastward and almost regularly rotate clockwise toward the southwest. Two opposite directions are observed in the evening. The summer and spring vector diagrams generally agree with the daily behavior of the velocity vector in autumn and winter. The directions are slightly more variable at night, and

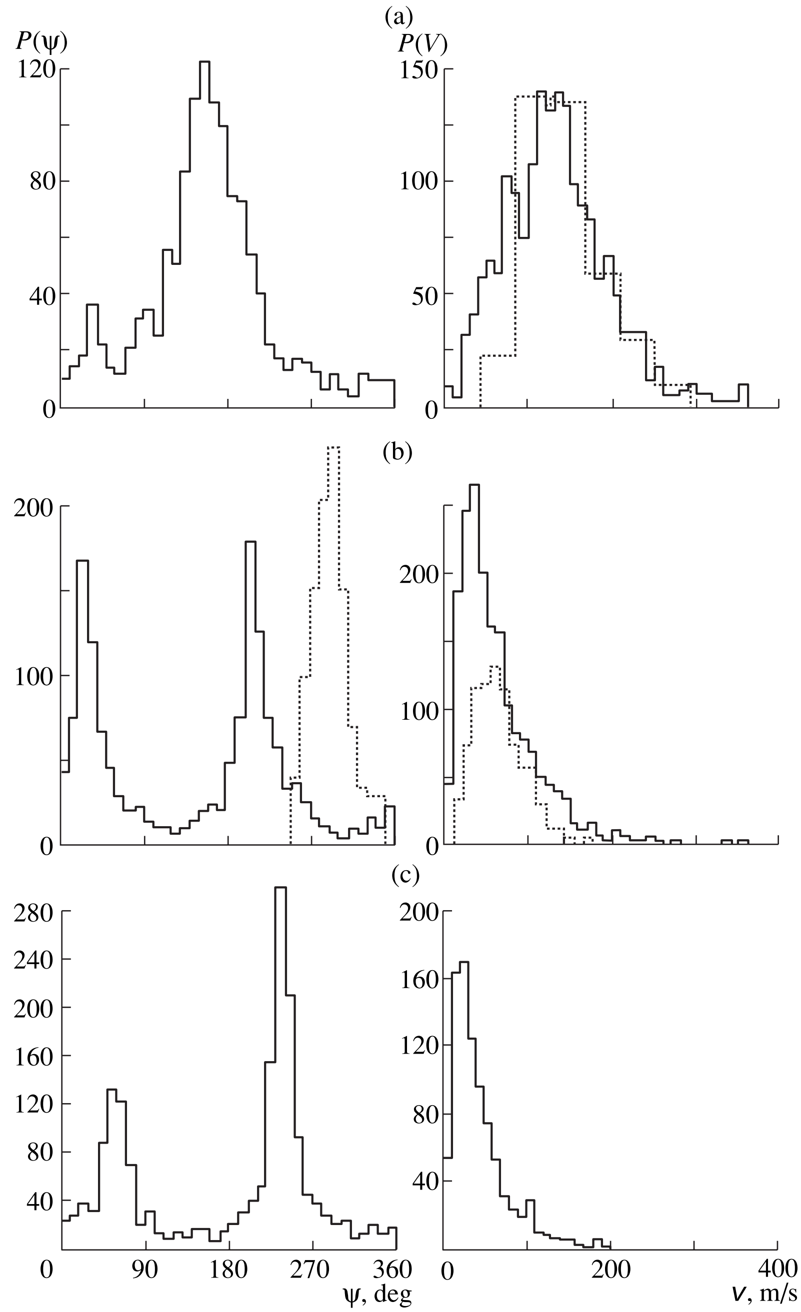


**Fig. 2.** Total distributions of azimuths (left panels) and velocities (right panels) constructed for: (a) daytime (08.00–16.00 LT); (b) night (20.00–04.00 LT) by the data of the phase measurements during 115 days in 1989–1990; (c) night-time by the measurements of amplitude scintillation characteristics. The data of diurnal measurements [25] are shown as a dotted line in Fig. 2a, right plate. The data of nocturnal measurements [26] are plotted as dotted lines in Fig. 2b.

the velocity vector rotation is less regular during daylight hours.

Both the $P(V)$ distribution form and average velocity vary smoothly in the winter and autumn. The most probable night value of $V$ does not exceed 30 m/s, averaging ~60 m/s. In the morning, the distribution form starts changing monotonically (it becomes more symmetric), and $V$ increases up to ~130 m/s. A virtually symmetric opposite process starts in the afternoon. The forms of $P(V)$ distributions in the summer and spring are close to those in the autumn and winter, but the night velocities are higher.

Different averaged models were used in earlier publications devoted to experimental verification of AGW filtering by the night wind [1–10]. For a comparison, we used a model that enabled us to calculate a neutral-wind velocity for arbitrary daytime with allowance for the magnetic activity index [19].

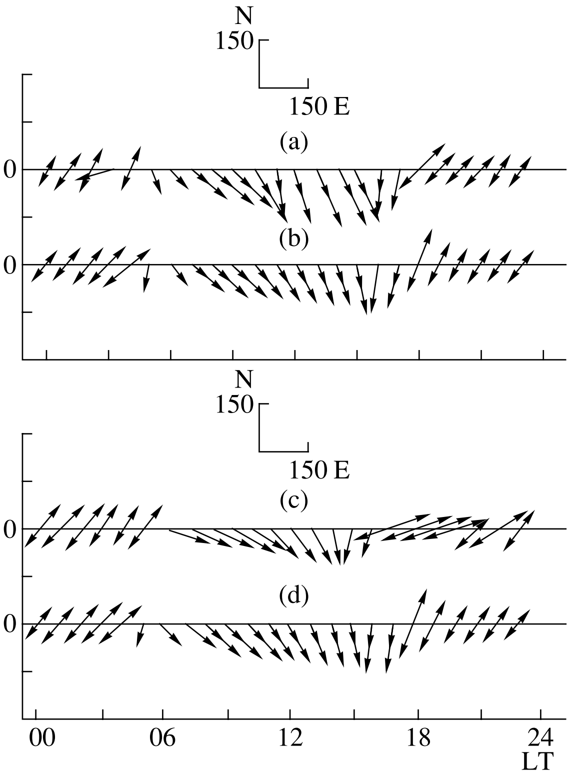


**Fig. 3.** Hourly vector values of azimuth and velocity averaged for the seasons: (a) winter, (b) autumn, (c) spring, (d) summer. An arrow length corresponds to an absolute velocity value.

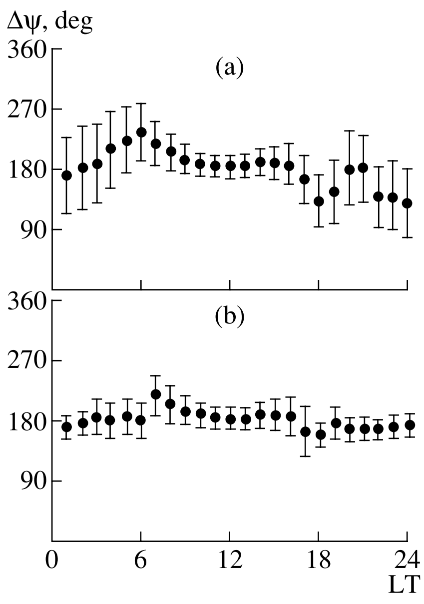


**Fig. 4.** Results of comparison between the hourly values of the phase front direction and the neutral wind direction, measured during 60 days in the autumn and winter seasons of 1989–1990 for: (a) complete days; (b) the daylight hours (06.00–18.00 LT). For night hours (18.00–06.00 LT, Fig. 4a), a comparison is made with the normal to the geomagnetic vector projection in the receiving antenna plane.

In Fig. 4, the hourly values of the phase-front directions during 60 days in the autumn and winter seasons of 1989–1990 are compared (according to the model [19]) with the neutral wind direction (for the daytime) and the normal to the geomagnetic vector projection in the receiving antenna plane (for night). In this sampling, the values of the geomagnetic activity index $K_p$ were not higher than 4.0.

Figure 4a shows the differences $\Delta\psi$ in directions between disturbances and wind. The values of root-mean-square deviations are plotted as vertical lines.

In the daytime, the $\Delta\psi$ value averages 180° with a root-mean-square deviation of ~15° were obtained for the entire data body. This is far more reliable (than it was established previously) evidence that the medium-scale displacements of ionization irregularities in the ionospheric $F2$ region are directed against the neutral wind.

However, the night experiment is considerably different from the filtering model (Fig. 4a). If we accept the previously formulated hypothesis that night medium-scale irregularities are extremely magnetized, the experimental and model data will be much closer. To illustrate this conclusion, we show the differences between the measured directions of travel and the normal to the magnetic vector projection in the plane of the receiving antenna array, reduced to 180° (Fig. 4b, from 18 to 06 LT). As a result, the difference between measured and calculated directions averages 180° with a root-mean-square deviation of ~9° for the entire data body.

## DISCUSSION

Our results for daytime agree well with the TID velocities and directions measured in vertical sounding [2, 3, 5, 6, 20–22] and with the data of transionospheric measurements [4, 7–10, 23, 24]. For a comparison, the well known $P(v)$ distribution [25] is plotted as a dotted line in Fig. 2a.

The published data of TID velocities $v$ measured at night do not allow one to distinguish any regularity in the variation of the travel direction [4–6, 9, 10, 21, 23]. The spaced ionosonde measurements and simultaneous night-time recording of $F$ scattering give velocity values close to our data; the results obtained in [26] on the basis of 2400 measurements are shown as $P(v)$ distribution in Fig. 2b (right panel, dotted line). The night-time TID velocities during $F$ scattering were 30–50 m/s, according to the antenna array measurements in Australia [27]. The night-time TID directions measured in Australia fall within an azimuth sector of 290°–310° [26–29]; the data from [26] are given for a comparison (Fig. 2b, left plate).

A large body of data on TID dynamics were obtained in the USA (36° N, 106° E) during a 500-day continuous cycle of measurements (1993–1994), using a radio interferometer with a large base (50–100 km) and recording the 137-MHz signal from the geostationary satellite *GEOS 2* [9]. For 08–16 LT in the spring and autumn periods, these data quite well agree with our data on TID rotation from the southeast to the southwest. It is interesting that the data referred to in [9] find their logical continuation on the interval 16–22 LT. Here, we see a tendency toward the azimuth displacement in the sector south-southwest (16–18 LT), southwest-west (18–20 LT), and west-northwest (20–22 LT).

The new results of measurements of AGW characteristics, with the use of radio heliograph (Nancy, France, 47.3° N, 2.2° E), are cited in [10], where the data of almost 800-hour observations of non-solar and solar radiation sources are analyzed. The directions of TID propagation are rather variable, the southern direction being predominant. Southeastward (in the daytime) and southwestward (at night) directions are distinguished in the daily distribution of averaged TID azimuths. Our daily data well agree with the data from [10], including a distinct change in directions from southeastward to southwestward ones. If the arguments for a southwestward (rather than a northeastward) direction, cited in [10], are used in the interpretation of our night-time data, the data from [10] will be virtually coincident with the corresponding data of our measurements on the entire daily interval.

We should note that the authors of [9, 10] do not think that their data reliably corroborate the hypothesis that TID are filtered by neutral winds. Therefore, it seems to be of current concern to continue experimenting with radio sounding facilities using both reflected and transionospheric radio signals.

## CONCLUSION

The above data on medium-scale TID dynamics during daylight hours are in virtual agreement with the hypothesis that AGW are filtered by the neutral wind. The assumption that similar medium-scale disturbances, detected at night during transionospheric sounding, are frozen in the magnetic field as small-scale ones (rather than being governed by the neutral wind), seems also to be substantiated.

It is also interesting that a night value of medium-scale TID directions is usually 10°–15° smaller than the corresponding value of small-scale irregularities, which (as expected) coincides with the normal to the magnetic vector shadow in the antenna array plane.

These effects are most pronounced in the winter and autumn and are almost independent of the magnetic activity level (up to $K_p = 5$).

## ACKNOWLEDGMENTS

We are grateful to N.P. Minko for his assistance in primary data processing, V.D. Kokourov for his constant interest and support in the course of this work, and V.M. Polyakov and N.N. Klimov for useful discussion.

This work was partially supported by the Russian Foundation for Basic Research, project nos. 93-05-9764 and 96-05-64162.

## REFERENCES

1. Kalikhman, A.D., Experimental Evidence for Filtering in the Direction of Medium-Scale Traveling Ionospheric Disturbances, *Geomagn. Aeron.*, 1978, vol. 18, no. 2, p. 358.
2. Kalikhman, A.D., Medium-Scale Traveling Ionospheric Disturbances and Thermospheric Winds in the *F* Region, *J. Atmos. Terr. Phys.*, 1980, vol. 42, no. 8, p. 697.
3. Morton, F.W. and Essex, E.A., Gravity Wave Observations at a Southern Hemisphere Mid-Latitude Station Using the Total Electron Content Technique, *J. Atmos. Terr. Phys.*, 1978, vol. 40, no. 10/11, p. 1113.
4. Waldock, J.A. and Jones, T.B., HF Doppler Observations of Medium-Scale Traveling Ionospheric Disturbances at Mid-Latitudes, *J. Atmos. Terr. Phys.*, 1986, vol. 48, no. 3, p. 245.
5. Crowley, G., Jones, T.B., and Dudeney, J.R., Comparison of Short Period TID Morphologies in Antarctica during Geomagnetically Quiet and Active Intervals, *J. Atmos. Terr. Phys.*, 1987, vol. 49, no. 11/12, p. 1155.
6. Morgan, M.G., Daytime Travelling Ionospheric Disturbances Observed at $L = 4.5$ in Western Quebec with Rapid-Run Ionosondes, *Radio Sci.*, 1990, vol. 25, no. 1, p. 73.
7. Mercier, C., Observations of Atmospheric Gravity Waves by Radiointerferometry, *J. Atmos. Terr. Phys.*, 1986, vol. 48, no. 7, p. 605.
8. Velthoven, P.F.J., Mercier, C., and Kelder, H., Simultaneous Observations of Traveling Ionospheric Disturbances by Two-Dimensional Radio Interferometry and the Differential Doppler Technique Applied to Satellite Signals, *J. Atmos. Terr. Phys.*, 1990, vol. 52, no. 4, p. 305.
9. Jacobson, A.R., Carlos, R.C., Massey, R.S., and Guang-hui, Wu, Observations of Traveling Ionospheric Disturbances with a Satellite-Beacon Radio Interferometer: Seasonal and Local-Time Behavior, *J. Geophys. Res.*, 1995, vol. 100, no. A2, p. 1653.
10. Mercier, C., Some Characteristics of Atmospheric Gravity Waves Observed by Radio-Interferometry, *Ann. Geophys.*, 1996, vol. 14, no. 1, p. 42.
11. Sinno, K. and Minakoshi, H., Experimental Results on Satellite Scintillations due to Field-Aligned Irregularities at Mid-Latitudes, *J. Atmos. Terr. Phys.*, 1983, vol. 45, no. 8/9, p. 563.
12. Kumagai, H., Behavior of Mid-Latitude *F*-Region Irregularities Deduced from Spaced-Receiver VHF Scintillation Measurements, *J. Atmos. Terr. Phys.*, 1986, vol. 48, no. 2, p. 221.
13. MacDougall, J.W., Elongation of Mid-Latitude Scintillation Irregularities, *J. Atmos. Terr. Phys.*, 1990, vol. 52, no. 2, p. 151.
14. Jacobson, A.R. and Erickson, W.C., Observations of Electron Density Irregularities in the Plasmosphere Using the VLA Radio Interferometer, *Ann. Geophys.*, 1993, vol. 11, no. 10, p. 869.

15. Bowman, G.G. and Hajkowicz, L.A., Small-Scale Ionospheric Structures Associated with Mid-Latitude Spread-*F*, *J. Atmos. Terr. Phys.*, 1991, vol. 53, no. 5, p. 447.
16. Afraimovich, E.L., Zvezdin, V.N., Minko, N.P., and Shapovalov, A.N., Simultaneous Measurements of the Polarization, Angles of Arrival, Doppler Frequency, and Amplitude of the VHF Radio Signal from *ETS-2*, *Radio Sci.*, 1991, vol. 26, no. 5, p. 1177.
17. Afraimovich, E.L., Dynamics and Anisotropy of Traveling Ionospheric Disturbances as Deduced from Transionospheric Sounding Data. I—Statistical Angle-of-Arrival and Doppler Method (SADM), *Preprint of Inst. of Solar and Terrestrial Physics, Russ. Acad. Sci.*, 1995, no. 5-95, p. 54.
18. Afraimovich, E.L., Boitman, O.N., Zhovty, E.I., and Kalikhman, A.D., Dynamics and Anisotropy of Traveling Ionospheric Disturbances as Deduced from Transionospheric Sounding Data. II. The Diurnal and Seasonal Statistic of Medium-Scale TIDs; the Neutral Wind and the Magnetic Field, *Preprint of Inst. of Solar and Terrestrial Physics, Russ. Acad. Sci.*, 1995, no. 6-95, p. 82.
19. Zhovty, E.I. and Chernigovskaya, M.A., Model of Large-Scale Motions and Electric Fields in the Mid- and Low-Latitude Ionosphere, *Issledovanie dinamicheskikh protsessov v verkhnei atmosfere* (Study of Dynamic Processes in the Upper Atmosphere), Moscow: Gidrometeoizdat, 1988, p. 267.
20. Afraimovich, E.L., Vugmeister, B.O., and Kalikhman, A.D., Comparison of Thermospheric Wind Dynamics Using Transionospheric and Vertical-Incidence Radio Sounding Data, *Adv. Space Res.*, 1996, vol. 18, no. 3, p. 121.
21. Drobzhev, V.I., Kaliev, M.Z., Krasnikov, I.M., *et al.*, Phase Velocities of Medium-Scale Wave Ionospheric Disturbances, *Geomagn. Aeron.*, 1988, vol. 28, no. 2, p. 308.
22. Afraimovich, E.L., Vugmeister, B.O., Zakharov, V.N., *et al.*, Experimental Study of Fluctuations of Doppler Frequencies and Arrival Angles of Radio Signal during Vertical Sounding of the Ionospheric *F*2 Layer, *Izv. Vyssh. Uchebn. Zaved., Radiofiz.*, 1978, vol. 21, no. 3, p. 338.
23. Afraimovich, E.L., Minko, N.P., and Fridman, S.V., Spectral and Dispersion Characteristics of Medium-Scale Traveling Ionospheric Disturbances as Deduced from Transionospheric Sounding Data, *J. Atmos. Terr. Phys.*, 1994, vol. 56, no. 11, p. 1431.
24. Kelder, H. and Spoelstra, T.A.Th., Medium Scale TIDs Observed by Radio Interferometry and Differential Doppler Techniques, *J. Atmos. Terr. Phys.*, 1987, vol. 49, no. 1, p. 7.
25. Munro, G.H., Traveling Disturbances in the *F*-Region, *Austral. J. Phys.*, 1958, vol. 11, no. 1, p. 91.
26. McNicol, R.W.E., Webster, H.S., and Bowman, G.G., A Study of Spread-*F* Ionospheric Echoes at Night at Brisbane. I—Range Spreading (Experimental), *Austral. J. Phys.*, 1956, vol. 9, no. 2, p. 247.
27. From, W.R. and Meehan, D.H., Mid-Latitude Spread-*F* Structure, *J. Atmos. Terr. Phys.*, 1988, vol. 50, no. 7, p. 629.